

Unit Ball Model for Hierarchical Embeddings in Complex Hyperbolic Space

Huiru Xiao¹ Caigao Jiang² Yangqiu Song¹ James Zhang² Junwu Xiong²

Abstract

Learning the representation of data with hierarchical structures in the hyperbolic space attracts increasing attention in recent years. Due to the constant negative curvature, the hyperbolic space resembles tree metrics and captures the tree-like properties of hierarchical graphs naturally, which enables the hyperbolic embeddings to improve over traditional Euclidean models. However, most graph data, even the data with hierarchical structures are not trees and they usually do not ubiquitously match the constant curvature property of the hyperbolic space. To address this limitation of hyperbolic embeddings, we explore the complex hyperbolic space, which has the variable negative curvature, for representation learning. Specifically, we propose to learn the graph embeddings in the unit ball model of the complex hyperbolic space. The unit ball model based embeddings have a more powerful representation capacity to capture a variety of hierarchical graph structures. Through experiments on synthetic and real-world data, we show that our approach improves over the hyperbolic embedding models significantly.

1. Introduction

Representation learning of data with hierarchical structures is an important machine learning task with many applications, such as taxonomy induction (Fu et al., 2014) and hypernymy detection (Shwartz et al., 2016). A popular methodology is to embed the data into continuous spaces whose geometrical properties fulfill the data structures. Traditional models (Nickel et al., 2011; Bordes et al., 2013) usually embed the data in the Euclidean space and are further improved by utilizing the complex Euclidean space (Trouillon et al., 2016; Sun et al., 2019). These models benefit from the vectorial structure and efficient computations in the Euclidean space. However, for data with hierarchical

structures such as taxonomies, the Euclidean space requires a large dimensionality to model the tree-like properties. It is shown that arbitrary tree structures cannot be embedded with arbitrary low distortion in the Euclidean space with an unbounded number of dimensions (Linial et al., 1995).

To exploit the structural property for learning the embeddings of hierarchical data, Nickel & Kiela (2017) embed the hierarchical graphs using the Poincaré ball model in the hyperbolic space. The hyperbolic space has constant negative curvature, which produces several manifestations. The most desirable property is that the hyperbolic space can be regarded as a continuous approximation to trees (Krioukov et al., 2010). The hyperbolic space is capable of embedding any finite tree while preserving the distances approximately (Gromov, 1987). As a result of the tree-like properties, the hyperbolic space is more suitable to embed data with underlying hierarchical structures than Euclidean space. The hyperbolic embeddings have been further improved (Ganea et al., 2018; Nickel & Kiela, 2018) and showed empirical success.

Nonetheless, the hierarchical graph data are usually different from trees in the sense that they can have complicated and varying local structures while being hierarchical globally. Thus, many general hierarchical graphs cannot ubiquitously match the constant negative curvature property of the hyperbolic space. To address the challenge, Gu et al. (2019) proposed to learn graph embeddings in a product manifold combining multiple spaces with different curvatures. Another possible solution is the trainable curvature, which is applied in other fields such as multi-relational graph embeddings (Chami et al., 2020) or graph neural network (Chami et al., 2019). These works use additional parameterization and more complicated models to compensate for the disparity between the actual data structures and the hyperbolic space.

In this paper, we present a new approach to learning the embeddings of hierarchical graphs. Specifically, we embed graph data into the unit ball model of the complex hyperbolic space, where the unit ball model is a projective geometry based model to identify the complex hyperbolic space. One of the main differences between the complex and the real hyperbolic space is that the curvature is no longer constant in the complex hyperbolic space, instead, it is vari-

¹Hong Kong University of Science and Technology ²Ant Group.
Correspondence to: Huiru Xiao <hxiaoaf@cse.ust.hk>.

able negative. In practice, the variable negative curvature makes our embeddings more flexible in handling varying structures while the tree-like properties retain the superiority in hierarchies. Furthermore, our proposed unit ball embedding approach does not need additional parameterization or special efforts to train the curvature. Through experiments on both synthetic and real-world data, we demonstrate the advantages of our approach. To summarize, our work has the following main contributions:

1. We present a novel embedding approach, which capitalizes on the variable negative curvature of the complex hyperbolic space, to handle noisier and more flexible hierarchies. To the best of our knowledge, our work is the first to propose complex hyperbolic embeddings.
2. We introduce the embedding algorithm in the unit ball model of the complex hyperbolic space. We formulate the learning and Riemannian optimization in the unit ball model.
3. We evaluate our approach with experiments on an extensive range of synthetic and real-world data and show the remarkable improvements of our approach.

2. Related Work

Hyperbolic embeddings. Hyperbolic embedding methods have become the leading approach for learning hierarchical embeddings. Nickel & Kiela (2017) learned the representations of the weighted graphs in the Poincaré ball model of the hyperbolic space and obtained high-quality embeddings for taxonomies. Ganea et al. (2018) introduced the hyperbolic entailment cones to formally define the partial ordering relation. Meanwhile, Nickel & Kiela (2018) proposed to learn the embeddings in the hyperboloid model (also known as the Lorentz model), another model of the hyperbolic space, which is isometric with the Poincaré ball model but has more simple metric and distance function to avoid the numerical instabilities. Additionally, the Riemannian version of adaptive optimization methods was developed by Bécigneul & Ganea (2019) to better optimize the hyperbolic embeddings. Yu & Sa (2019) used an integer-based tiling to solve the numerical instabilities.

Instead of the above optimization-based methods, another branch of hyperbolic embeddings studies the combinatorial construction-based methods (Sala et al., 2018; Sonthalia & Gilbert, 2020), which targeted constructing tree structures from data in the hyperbolic space. Gu et al. (2019) extended the construction-based hyperbolic embeddings in the geometric learning framework. Specifically, it proposed to jointly learn the curvature of the data structures and the data embeddings in a product manifold combining spherical manifold (\mathbb{S}), hyperbolic manifold (\mathbb{H}), and Euclidean

manifold (\mathbb{E}). Nevertheless, the search space for each graph is enormous. For instance, if we want to embed a graph into the 10-dimensional product manifold, the possible combinations include \mathbb{E}^{10} , $\mathbb{H}^5 \times \mathbb{S}^5$, $(\mathbb{H}^2)^2 \times \mathbb{E}^2 \times (\mathbb{S}^2)^2$, etc, which makes it impractical to search for the best manifold combination for each new graph.

Note that our complex hyperbolic embedding model is different from the hyperbolic embedding methods (Nickel & Kiela, 2017; 2018) or the embeddings in the product space (Gu et al., 2019) since the geometrical spaces are typically of different characteristics. The n -dimensional (n -d) complex hyperbolic space is not simply the $2n$ -d hyperbolic space or the product of two n -d hyperbolic spaces. Section 3 will show that the hyperbolic and the complex hyperbolic space differ markedly in geometry.

Motivated by the promising results of previous works, the extensions to the multi-relational graph hyperbolic embeddings (Balazevic et al., 2019; Chami et al., 2020; Sun et al., 2020) were explored by using different relational parameterization models in the hyperbolic space. Since we only focus on the single-relation graph embeddings and taxonomy embeddings in this work, we do not evaluate the multi-relational knowledge graph embedding models in our tasks.

Complex embeddings. The traditional knowledge graph embeddings were learned in the real Euclidean space (Nickel et al., 2011; Bordes et al., 2013; Yang et al., 2015) and were used for knowledge graph inference and reasoning. In the past few years, several works suggested utilizing the complex Euclidean space for inferring more relation patterns. ComplEx (Trouillon et al., 2016) found that the Hermitian dot product of the complex space effectively captures anti-symmetric relations while retaining the efficiency benefits of the dot product. RotatE (Sun et al., 2019) defined each relation as a rotation in the complex Euclidean space to infer various relation patterns. The Hermitian dot product and rotation are simple computation operations and transformations in the complex space, whereas they have been demonstrated to be effective in the knowledge graph embeddings. The success of the complex embeddings reveals the potential of the complex space and inspires us to explore the complex hyperbolic space.

3. Preliminaries

3.1. Basic Definitions

Before introducing the hyperbolic geometry and the complex hyperbolic geometry, we need to explain and define some related concepts. The first one is *curvature*, which describes the curve of Riemannian manifolds and controls the rate of geodesic deviation. In this paper, *curvature* refers to the *sectional curvature*.

Table 1. Comparison of Euclidean, hyperbolic, and complex hyperbolic geometries. n denotes the dimensionality.

	Curvature	Volume growth of ball of radius ρ
Euclidean	0 (constant)	$\sim \rho^n$ (polynomially)
Hyperbolic	$K < 0$ (constant negative)	$\sim e^{\sqrt{-K}(n-1)\rho}$ (exponentially)
Complex hyperbolic	pinched between -1 and $-\frac{1}{4}$ (variable negative)	$\sim e^{n\rho}$ (exponentially)

Definition 1 (Curvature). *Given a Riemannian manifold and two linearly independent tangent vectors at the same point, \mathbf{u} and \mathbf{v} , the (sectional) curvature is defined as*

$$K(\mathbf{u}, \mathbf{v}) = \frac{\langle R(\mathbf{u}, \mathbf{v})\mathbf{v}, \mathbf{u} \rangle}{\langle \mathbf{u}, \mathbf{u} \rangle \langle \mathbf{v}, \mathbf{v} \rangle - \langle \mathbf{u}, \mathbf{v} \rangle^2},$$

where R is the Riemann curvature tensor, defined by the convention $R(\mathbf{u}, \mathbf{v})\mathbf{w} = \nabla_{\mathbf{u}}\nabla_{\mathbf{v}}\mathbf{w} - \nabla_{\mathbf{v}}\nabla_{\mathbf{u}}\mathbf{w} - \nabla_{[\mathbf{u}, \mathbf{v}]}\mathbf{w}$.

Next, we give the definition of δ -hyperbolicity (Gromov, 1987), which measures the tree-likeness of graphs. The lower δ corresponds to the more tree-like graph. Trees have 0 δ -hyperbolicity. The metric will be used to analyze the datasets in Section 5.

Definition 2 (δ -hyperbolicity). *Let a, b, c, d be vertices of the graph G . Let S_1, S_2 and S_3 be*

$$\begin{aligned} S_1 &= \text{dist}(a, b) + \text{dist}(d, c), \\ S_2 &= \text{dist}(a, c) + \text{dist}(b, d), \\ S_3 &= \text{dist}(a, d) + \text{dist}(b, c). \end{aligned}$$

Suppose M_1 and M_2 are the two largest values among S_1, S_2, S_3 and $M_1 \geq M_2$. Define $\text{hyp}(a, b, c, d) = M_1 - M_2$. Then the δ -hyperbolicity of G is defined as

$$\delta(G) = \frac{1}{2} \max_{a, b, c, d \in V(G)} \text{hyp}(a, b, c, d).$$

That is, $\delta(G)$ is the maximum of hyp over all possible 4-tuples (a, b, c, d) divided by 2.

3.2. Hyperbolic Geometry

Hyperbolic space¹ is a homogeneous space with constant negative curvature. Here *constant* means constant both at all points and in all pairs of directions. There are several models of the hyperbolic space (Cannon et al., 1997) to describe it in mathematical language. For representation learning, the Poincaré ball model (Nickel & Kiela, 2017) and the hyperboloid model (the Lorentz model) (Nickel & Kiela, 2018) are widely used. The hyperbolic distance has the desirable property of resemblance to tree metrics. Specifically, the closer a point is to the origin, the smaller distances it has

¹In this paper, we use *hyperbolic space* to refer to real hyperbolic space and *hyperbolic embeddings* to refer to real hyperbolic embeddings for avoiding wordiness.

to other points. Conversely, the points near the boundary have comparatively large distances from each other. Let's consider the tree structure, where the root node has relatively small distances to other nodes while leaf nodes are usually farther away from each other. Krioukov et al. (2010) built the approximate equivalence between hierarchical networks and the hyperbolic space.

3.3. Complex Hyperbolic Geometry

Complex hyperbolic space is a homogeneous geometry of variable negative curvature. Its ambient Hermitian vector space $\mathbb{C}^{n,1}$ is the complex Euclidean space \mathbb{C}^{n+1} endowed with a Hermitian form $\langle \mathbf{z}, \mathbf{w} \rangle$, where $\mathbf{z}, \mathbf{w} \in \mathbb{C}^{n+1}$. Then the Hermitian space $\mathbb{C}^{n,1}$ can be divided into three subsets: $V_- = \{\mathbf{z} \in \mathbb{C}^{n,1} | \langle \mathbf{z}, \mathbf{z} \rangle < 0\}$, $V_0 = \{\mathbf{z} \in \mathbb{C}^{n,1} | \langle \mathbf{z}, \mathbf{z} \rangle = 0\}$, and $V_+ = \{\mathbf{z} \in \mathbb{C}^{n,1} | \langle \mathbf{z}, \mathbf{z} \rangle > 0\}$. Let \mathbb{P} be a projection map $\mathbb{P} : \mathbb{C}^{n,1} - \{z_{n+1} = 0\} \rightarrow \mathbb{C}^n$

$$\mathbb{P} : \begin{bmatrix} z_1 \\ \vdots \\ z_{n+1} \end{bmatrix} \mapsto \begin{bmatrix} z_1/z_{n+1} \\ \vdots \\ z_n/z_{n+1} \end{bmatrix}. \quad (1)$$

Then the complex hyperbolic space $\mathbb{H}_{\mathbb{C}}^n$ and its boundary $\partial\mathbb{H}_{\mathbb{C}}^n$ are defined using the projectivization:

$$\mathbb{H}_{\mathbb{C}}^n = \mathbb{P}V_-, \quad \partial\mathbb{H}_{\mathbb{C}}^n = \mathbb{P}V_0. \quad (2)$$

The curvature of the complex hyperbolic space is summarized by Goldman (1999) in the following theorem:

Theorem 1. *The curvature is not constant in $\mathbb{H}_{\mathbb{C}}^n$. It is pinched between -1 (in the directions of complex projective lines) and $-1/4$ (in the directions of totally real planes).*

We leave the full proof in the supplementary material. The non-constant curvature, which we expect to be favorable for embedding flexible hierarchical graphs, is one of the main differences between $\mathbb{H}_{\mathbb{C}}^n$ and the real hyperbolic space $\mathbb{H}_{\mathbb{R}}^n$.

The complex hyperbolic space also has the tree-like property that the volume of a ball grows exponentially with its radius. The volume of a ball with radius ρ in $\mathbb{H}_{\mathbb{C}}^n$ is given by

$$\text{vol}(B_{\mathbb{H}_{\mathbb{C}}^n}(\rho)) = \frac{8^n \sigma_{2n-1}}{2n} \sinh^{2n}(\rho/2) \sim \frac{8^n \sigma_{2n-1}}{2n} e^{n\rho}, \quad (3)$$

where $\sigma_{2n-1} = 2\pi^n/n!$ is the Euclidean volume of the unit sphere $S^{2n-1} \in \mathbb{C}^n$. Thus the volume of a ball in $\mathbb{H}_{\mathbb{C}}^n$ has

exponential growth rate n . In contrast, in a real hyperbolic space $\mathbb{H}_{\mathbb{R}}^n(K)$ of dimension n and curvature $K < 0$, the volume of a ball with radius ρ grows like

$$\text{vol}(B_{\mathbb{H}_{\mathbb{R}}^n(K)}(\rho)) \sim e^{\sqrt{-K}(n-1)\rho}. \quad (4)$$

In particular, as shown in (Goldman, 1999), the exponential growth rate of volume in the totally geodesic subspace $\mathbb{H}_{\mathbb{R}}^n \in \mathbb{H}_{\mathbb{C}}^n$ is $(n-1)/2$ as compared with the exponential growth rate n of the ambient $\mathbb{H}_{\mathbb{C}}^n$. Although having diverse exponential rates, the volume of a ball grows exponentially with its radius both in complex hyperbolic space and hyperbolic space. The property is highly tree-like since the number of nodes grows exponentially with depth of a tree.

Contrastively, the volume of a ball in Euclidean space \mathbb{E}^n grows polynomially with its radius:

$$\text{vol}(B_{\mathbb{E}^n}(\rho)) = \frac{\pi^{\frac{n}{2}}}{\Gamma(\frac{n}{2})} \rho^n \sim \rho^n. \quad (5)$$

In summary, Table 1 outlines our concerned properties of Euclidean, hyperbolic, and complex hyperbolic geometry.

4. Unit Ball Embeddings

We propose to embed the graph data into the unit ball model of the complex hyperbolic space. In this section, We introduce our approach in detail.

4.1. The Unit Ball Model

The unit ball model is used to identify the complex hyperbolic space, which can be derived via the projective geometry (Goldman, 1999). We now provide the brief derivation sketch and some basic formulas.

Take the Hermitian form of $\mathbb{C}^{n,1}$ in Section 3.3 to be a standard Hermitian form:

$$\langle \mathbf{z}, \mathbf{w} \rangle = z_1 \bar{w}_1 + \cdots + z_n \bar{w}_n - z_{n+1} \bar{w}_{n+1}. \quad (6)$$

Take $z_{n+1} = 1$ in the projection map \mathbb{P} (Eq. (1)), then from Eq. (2), we can derive the formula of the unit ball model:

$$\mathcal{B}_{\mathbb{C}}^n = \{(z_1, \dots, z_n, 1) \mid |z_1|^2 + \cdots + |z_n|^2 < 1\}, \quad (7)$$

where $|\cdot|$ is the Euclidean norm.

The metric on $\mathcal{B}_{\mathbb{C}}^n$ is Bergman metric, which takes the formula below in 2-d case:

$$ds^2 = \frac{-4}{\langle \mathbf{z}, \mathbf{z} \rangle^2} \det \begin{bmatrix} \langle \mathbf{z}, \mathbf{z} \rangle & \langle d\mathbf{z}, \mathbf{z} \rangle \\ \langle \mathbf{z}, d\mathbf{z} \rangle & \langle d\mathbf{z}, d\mathbf{z} \rangle \end{bmatrix}. \quad (8)$$

The distance function on $\mathcal{B}_{\mathbb{C}}^n$ is given by

$$d_{\mathcal{B}_{\mathbb{C}}^n}(\mathbf{z}, \mathbf{w}) = \text{arcosh}(2 \frac{\langle \mathbf{z}, \mathbf{w} \rangle \langle \mathbf{w}, \mathbf{z} \rangle}{\langle \mathbf{z}, \mathbf{z} \rangle \langle \mathbf{w}, \mathbf{w} \rangle} - 1), \quad (9)$$

where the Hermitian form $\langle \mathbf{z}, \mathbf{w} \rangle$ is defined in Eq. (6).

4.2. Embedding Graphs in the Unit Ball Model

Given a graph containing a set of nodes $X = \{x_p\}_{p=1}^m$ and a set of edges $E = \{(x_p, x_q) \mid x_p, x_q \in X\}$, we aim to learn the embeddings of the nodes $\mathbf{Z} = \{\mathbf{z}_p\}_{p=1}^m$, where $\mathbf{z}_p \in \mathcal{B}_{\mathbb{C}}^n$.

The objective of the embeddings is to recover the structures of the graph, including the distances between the nodes as well as the partial order in the hierarchies. Here we adopt the soft ranking loss used in the Poincaré ball embeddings (Nickel & Kiela, 2017) and the hyperboloid embeddings (Nickel & Kiela, 2018):

$$L = \sum_{(x_p, x_q) \in E} \log \frac{e^{-d_{\mathcal{B}_{\mathbb{C}}^n}(\mathbf{z}_p, \mathbf{z}_q)}}{\sum_{x_k \in \mathcal{N}(x_p)} e^{-d_{\mathcal{B}_{\mathbb{C}}^n}(\mathbf{z}_p, \mathbf{z}_k)}}, \quad (10)$$

where $\mathcal{N}(x_p) = \{x_k : (x_p, x_k) \notin E\} \cup \{x_p\}$ is the set of negative examples for x_p together with x_p . $d_{\mathcal{B}_{\mathbb{C}}^n}$ is the distance function in the unit ball model given in Eq. (9). The minimization of L makes the connected nodes closer in the embedding space than those with no observed edges.

Note that instead of manually setting the curvature of the learning space or training the curvature as extra parameters, we learn the embeddings directly in the complex hyperbolic space, where the curvature is variable. The learned embeddings are located in different submanifolds of the unit ball model. For example, they can be in the complex projective lines or the totally geodesic planes, then the curvature would be different, which is very useful to model data with diverse local structures.

4.3. Riemannian Optimization in the Unit Ball Model

In order to learn our proposed embeddings $\mathbf{Z} = \{\mathbf{z}_p\}_{p=1}^m$, we need to solve the optimization problem with constraint:

$$\mathbf{Z} \leftarrow \arg \min_{\mathbf{Z}} L \quad \text{s.t. } \forall \mathbf{z}_p \in \mathbf{Z}, \mathbf{z}_p \in \mathcal{B}_{\mathbb{C}}^n. \quad (11)$$

For the optimization problems in Riemannian manifolds, Bonnabel (2013) presented the Riemannian stochastic gradient descent (RSGD) algorithm, which we employ to optimize Eq. (11). To update an embedding $\mathbf{z} \in \mathcal{B}_{\mathbb{C}}^n$,² we need to obtain its Riemannian gradient (∇_R). Specifically, denote $\mathcal{T}_{\mathbf{z}}\mathcal{B}_{\mathbb{C}}^n$ as the tangent space of \mathbf{z} , then the embedding is updated at the t -th iteration as

$$\mathbf{z}^{(t)} \leftarrow \mathbf{z}^{(t-1)} - \eta^{(t)} \nabla_R L(\mathbf{z}), \quad (12)$$

where $\eta^{(t)}$ is the learning rate at the t -th iteration and $\nabla_R L(\mathbf{z}) \in \mathcal{T}_{\mathbf{z}}\mathcal{B}_{\mathbb{C}}^n$ is the Riemannian gradient of $L(\mathbf{z})$.

The Riemannian gradient ∇_R can be derived from rescaling the Euclidean gradient ∇_E with the inverse of the metric

²Here we omit the subscript of \mathbf{z}_p for concision.

Algorithm 1 RSGD of the Unit Ball Embeddings

Input: initialization $\mathbf{z}^{(0)}$, number of iterations T , learning rates $\{\eta^{(t)}\}_{t=1}^T$.
for $t = 1$ **to** T **do**
 Compute $\frac{\partial d_{\mathcal{B}_{\mathbb{C}}^n}}{\partial \mathbf{x}}$ and $\frac{\partial d_{\mathcal{B}_{\mathbb{C}}^n}}{\partial \mathbf{y}}$ by Eqs. (17) and (18).
 Compute $\nabla_E L(\mathbf{z})$ by Eq. (14).
 Update $\mathbf{z}^{(t)}$ by Eq. (20).
end for

tensor ds^2 in Eq. (8):

$$\nabla_R L(\mathbf{z}) = \frac{1}{ds^2} \nabla_E L(\mathbf{z}). \quad (13)$$

Thus the problem converts to computing $\nabla_E L(\mathbf{z})$. Applying the chain rule of differential functions, we have

$$\nabla_E L(\mathbf{z}) = \frac{\partial L(\mathbf{z})}{\partial d_{\mathcal{B}_{\mathbb{C}}^n}(\mathbf{z}, \mathbf{w})} \nabla_E d_{\mathcal{B}_{\mathbb{C}}^n}(\mathbf{z}, \mathbf{w}), \quad (14)$$

where $\frac{\partial L(\mathbf{z})}{\partial d_{\mathcal{B}_{\mathbb{C}}^n}(\mathbf{z}, \mathbf{w})}$ is trivial to compute from Eq. (10).

In practical training, we implement and compute the complex embedding as its real part and imaginary part, i.e., $\mathbf{z} = \mathbf{x} + i\mathbf{y}$, where i represents the *imaginary unit*, satisfying $i^2 = -1$. Therefore, in order to get the gradient of the distance function $\nabla_E d_{\mathcal{B}_{\mathbb{C}}^n}(\mathbf{z}, \mathbf{w})$ in Eq. (14), we get the partial derivative with regard to the real part and the imaginary part, i.e., $\nabla_E d_{\mathcal{B}_{\mathbb{C}}^n}(\mathbf{z}, \mathbf{w}) = \frac{\partial d_{\mathcal{B}_{\mathbb{C}}^n}(\mathbf{z}, \mathbf{w})}{\partial \mathbf{x}} + i \frac{\partial d_{\mathcal{B}_{\mathbb{C}}^n}(\mathbf{z}, \mathbf{w})}{\partial \mathbf{y}}$.

According to the derivative of a complex function $f(z)$ at $z = x + iy$:

$$\frac{\partial f(z, \bar{z})}{\partial x} = \left(\frac{\partial}{\partial z} + \frac{\partial}{\partial \bar{z}} \right) f(z, \bar{z}), \quad (15)$$

$$\frac{\partial f(z, \bar{z})}{\partial y} = i \left(\frac{\partial}{\partial z} - \frac{\partial}{\partial \bar{z}} \right) f(z, \bar{z}), \quad (16)$$

where $\bar{z} = x - iy$ is the conjugate of z . We can obtain the partial derivatives of the unit ball model distance:

$$\frac{\partial d_{\mathcal{B}_{\mathbb{C}}^n}}{\partial \mathbf{x}} = \frac{4}{\sqrt{p^2 - 1}} \left(\frac{\text{Re}(\langle \mathbf{z}, \mathbf{w} \rangle \mathbf{w})}{\langle \mathbf{z}, \mathbf{z} \rangle \langle \mathbf{w}, \mathbf{w} \rangle} - \frac{\langle \mathbf{z}, \mathbf{w} \rangle \langle \mathbf{w}, \mathbf{z} \rangle \mathbf{x}}{\langle \mathbf{z}, \mathbf{z} \rangle^2 \langle \mathbf{w}, \mathbf{w} \rangle} \right), \quad (17)$$

$$\frac{\partial d_{\mathcal{B}_{\mathbb{C}}^n}}{\partial \mathbf{y}} = \frac{4}{\sqrt{p^2 - 1}} \left(\frac{\text{Im}(\langle \mathbf{z}, \mathbf{w} \rangle \mathbf{w})}{\langle \mathbf{z}, \mathbf{z} \rangle \langle \mathbf{w}, \mathbf{w} \rangle} - \frac{\langle \mathbf{z}, \mathbf{w} \rangle \langle \mathbf{w}, \mathbf{z} \rangle \mathbf{y}}{\langle \mathbf{z}, \mathbf{z} \rangle^2 \langle \mathbf{w}, \mathbf{w} \rangle} \right), \quad (18)$$

where $p = \cosh(d_{\mathcal{B}_{\mathbb{C}}^n}(\mathbf{z}, \mathbf{w}))$, $\text{Re}(\cdot)$ and $\text{Im}(\cdot)$ denote the real and the imaginary part respectively. The full derivation of Eq. (17) and (18) is given in the supplementary material.

Since the embedding \mathbf{z} should be constrained within the unit ball model, we apply the same projection strategy as (Nickel

& Kiela, 2017) via a small constant ε :

$$\text{proj}(\mathbf{z}) = \begin{cases} \mathbf{z}/(|\mathbf{z}| - \varepsilon) & \text{if } |\mathbf{z}| \geq 1, \\ \mathbf{z} & \text{otherwise.} \end{cases} \quad (19)$$

To sum up, the update of \mathbf{z} at the t -th iteration is

$$\mathbf{z}^{(t)} \leftarrow \text{proj}(\mathbf{z}^{(t-1)} - \eta^{(t)} \frac{1}{ds^2} \nabla_E L(\mathbf{z})). \quad (20)$$

The update steps of RSGD are presented in Algorithm 1.

5. Experiments

In this section, we evaluate the performances of our approach. We mainly focus on the tasks of graph reconstruction and link prediction, which evaluate the representation capacity and generalization performance respectively.

5.1. Experimental Settings

5.1.1. DATA

We use synthetic and real-world data that exhibit underlying hierarchical structure. The details are as follows.

Synthetic. We generate various balanced trees and compressed graphs using NetworkX package.³ For **balanced trees**, we generate the balanced tree with degree r and depth h . For **compressed graphs**, we generate k random trees on m nodes and then aggregate their edges to form a graph. Some examples are given in the supplementary material.

ICD10. The International Statistical Classification of Diseases and Related Health Problems⁴ (ICD) is a medical classification list provided by the World Health Organization. The classification list forms a tree structure. We construct the full transitive closure of the 10-th revision of ICD (ICD10) as our ICD10 dataset.

YAGO3-wikiObjects. YAGO3⁵ (Mahdisoltani et al., 2015) is a huge semantic knowledge base. It provides a taxonomy derived from Wikipedia and WordNet. We extract the Wikipedia concepts and entities that are descendants of $\langle \text{wikicat_Objects} \rangle$ as well as the hypernymy edges among them. We then compute the transitive closure of the sampled taxonomy to construct the YAGO3-wikiObjects dataset.

WordNet-noun. WordNet⁶ (Miller, 1995) is a large lexical database. The hypernymy relation among all nouns forms a hierarchy. We use the transitive closure of the noun hierarchy as our WordNet-noun dataset.

³<https://networkx.org/documentation/stable/reference/generators.html>

⁴<https://www.who.int/standards/classifications/classification-of-diseases>

⁵<https://yago-knowledge.org/>

⁶<https://wordnet.princeton.edu/>

For each real-world dataset, we randomly split the edges into train-validation-test sets with the ratio 90%:5%:5%. We make sure that any node in the validation and test set must occur in the training set since otherwise, it cannot be predicted. But the edges in the validation and test set do not occur in the training set since the three sets are disjoint. We provide the statistics of real-world datasets in Table 2.

5.1.2. TASKS

We focus on the following two tasks:

Graph reconstruction. We embed the data with the full graph as the training set and then reconstruct the graph (i.e., the full graph also as the test set) from the embeddings. The task evaluates representation capacity.

Link prediction. We train the embeddings on the training set and predict the edges in the test set, which evaluates generalization performance.

5.1.3. BASELINES

We compare our approach **UnitBall** to the following methods: (1) The combinatorial construction method for learning the hyperbolic representation **TreeRep** (Sonthalia & Gilbert, 2020). (2) The hyperbolic embeddings in the **Poincaré** ball model (Nickel & Kiela, 2017). (3) The hyperbolic embeddings in the **Hyperboloid** model (Nickel & Kiela, 2018). (4) The simple **Euclidean** embedding model using the same loss function with (Nickel & Kiela, 2017; 2018).

The first three baselines are embedding methods in the hyperbolic space, where the curvature is constant negative, while the fourth baseline learns in the Euclidean space with 0 curvature. As mentioned in Section 4.2, we use the same loss function with the Poincaré and hyperboloid embeddings but learn in the unit ball model of complex hyperbolic space. Therefore, the comparisons among UnitBall, Poincaré, Hyperboloid, and Euclidean demonstrate the representation capacities of different geometrical models in different spaces.

5.1.4. IMPLEMENTATION DETAILS

For the baselines, we use their public codes to train the embeddings. For all methods, we tune the hyperparameters on the validation sets for the link prediction task while tuning the hyperparameters on each full dataset for the graph reconstruction task. The hyperparameters are given in the supplementary material. In all experiments, we report the mean results over 5 running executions.

5.1.5. EVALUATION

We use the mean average precision (**MAP**), mean reciprocal rank (**MRR**), and the proportion of correct types that rank no larger than N (**Hits@N**) as our evaluation metrics, which

Table 2. Datasets statistics. δ -hyperbolicity is a metric to measure the tree-likeness of graphs, defined in Definition 2. The lower δ corresponds to the more tree-like graph.

	ICD10	wikiObjects	noun
Nodes	19,155	17,375	82,115
Edges	78,357	153,643	743,086
Depth	6	16	20
Training edges	70,521	138,277	668,776
Valid/Test edges	3,918	7,683	37,155
δ -hyperbolicity	0.0	1.0	0.5

are widely used for evaluating ranking and link prediction.

The n -dimensional (n -d) complex hyperbolic embeddings have around double parameters of the n -d real embeddings since the n -d complex hyperbolic vectors have n -d real part and n -d imaginary part. For a fair comparison, in each experimental setting, we compare our n -d complex hyperbolic embeddings of UnitBall against the $2n$ -d embeddings of all baselines. The results will also demonstrate that the n -d complex hyperbolic space is not simply the $2n$ -d hyperbolic space, they have different capacities.

5.2. Graph Reconstruction

5.2.1. RESULTS ON BALANCED TREES

To compare the representation capacities of UnitBall and other hyperbolic embedding models for the tree structures, we first evaluate on the graph reconstruction task using the synthetic balanced trees. A balanced tree- (r, h) has degree r and depth h , so it has $r^0 + \dots + r^d$ nodes and $r^0 + \dots + r^d - 1$ edges. The δ -hyperbolicity of any balanced tree is 0. We embed the balanced trees into 20-d hyperbolic space and 10-d complex hyperbolic space for UnitBall.

Figure 1 presents the MAP and Hits@3 scores with varying r and h . We see that when the tree is in small scale, e.g., $(r, h) = (15, 3), (10, 2), (10, 3)$, all methods have very good performances, demonstrating the expected powerful capacities of hyperbolic geometry and complex hyperbolic geometry on tree structures. However, when the breadth or the depth increases, the performances of Poincaré and Hyperboloid drop rapidly, suggesting that the optimization-based embeddings in $\mathbb{H}_{\mathbb{R}}^{20}$ are not effective enough for reconstructing trees of such scales.

In comparison, UnitBall and TreeRep achieve stable performances for larger trees. TreeRep gets slightly better results than UnitBall on $(r, h) = (20, 3)$ and $(10, 4)$. Note that TreeRep is the combinatorial construction-based method, which learns a tree structure from the data as an intermediate step and then embeds the learned trees into the hyperbolic space using Sarkar’s construction (Sarkar, 2011). In the case when the graph is a tree, i.e., δ -hyperbolicity = 0, TreeRep

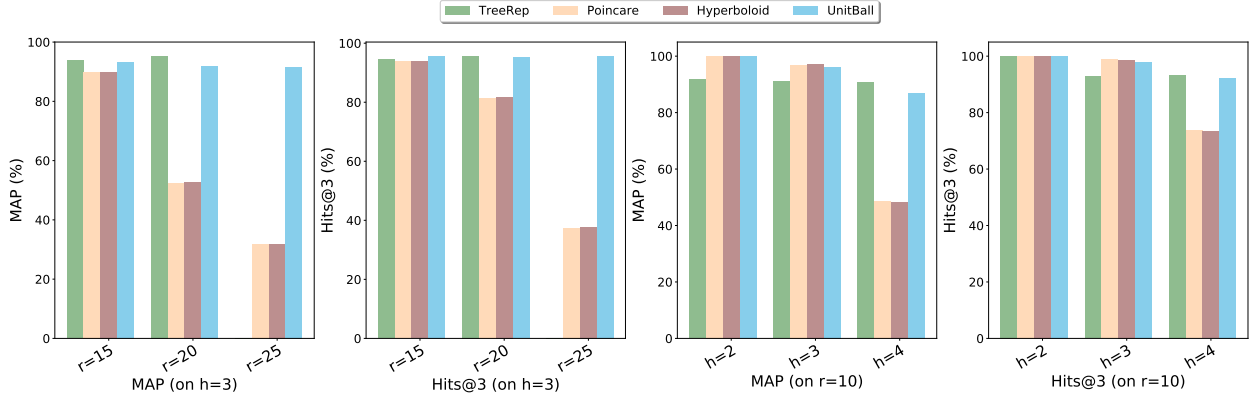


Figure 1. Evaluation of graph reconstruction on synthetic balanced trees in 20-d embedding spaces (10-d complex hyperbolic space for UnitBall). r represents the degree while h represents the depth. TreeRep is not applicable on $r = 25$ due to the large memory cost.

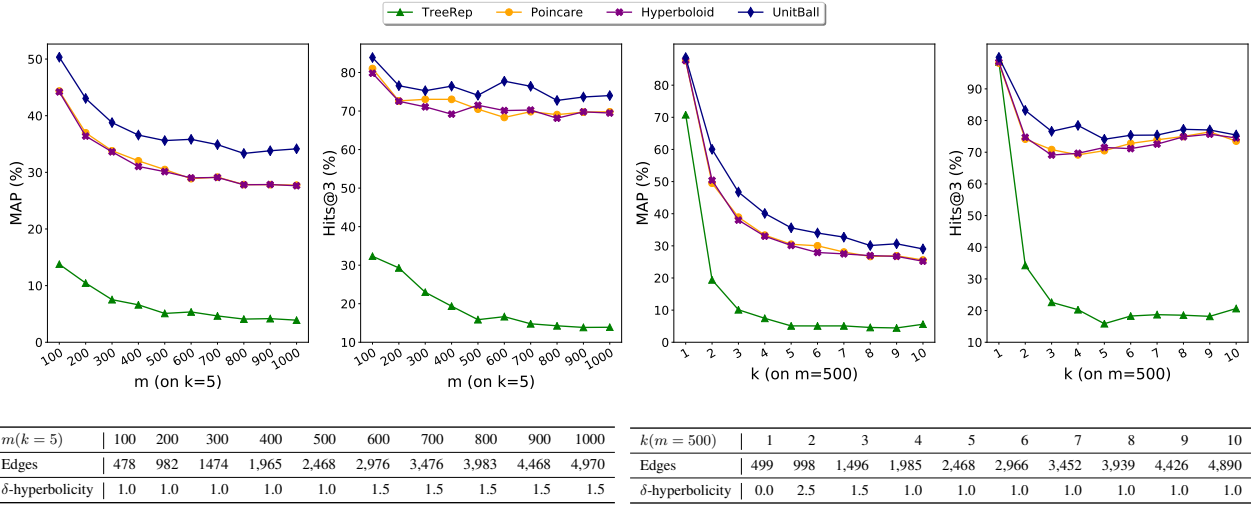


Figure 2. Evaluation of graph reconstruction on synthetic compressed graphs in 20-d embedding spaces (10-d complex hyperbolic space for UnitBall). m represents the number of nodes in the graph while k represents the number of random trees aggregated to the graph (k controls the denseness and noise level of the graph). The statistics of the compressed graphs are provided in the tables.

exactly recovers the original tree structure, which is why TreeRep can produce extremely high-quality results on balanced trees. Even so, UnitBall has very close performances with TreeRep on balanced trees, demonstrating the robustness and capacity of UnitBall. We will see that TreeRep is incapable of reconstructing the varying graph structures in Section 5.2.2. In addition, although TreeRep is very efficient in embedding tree structures since the construction-based method does not need the gradient-based optimization steps, it costs too much memory resource for constructing the tree structures from data. For a graph with m nodes, it needs to construct a shortest path metric matrix of size $m \times m$ before constructing the tree structure. The storage and the computations of the large matrix make TreeRep unscalable to large graphs such as balanced tree- $(r, h) = (25, 3)$.

5.2.2. RESULTS ON COMPRESSED GRAPHS

To illustrate the benefits of UnitBall on flexible graph structures other than trees, we now test on the compressed graphs. Each compressed graph- (m, k) consists of m nodes and is aggregated from k random trees on the m nodes. The bigger k corresponds to the denser and noisier graph.

Figure 2 depicts the reconstruction results as a function of varying m and k . The results on the compressed graphs are not as good as on balanced trees, especially with the increase of m and k , which represents the increase of graph scale and denseness respectively. Notably, UnitBall outperforms all other methods on these challenging data, showing that UnitBall handles the noisy tree-like graphs better. Similar to results on balanced trees, Poincaré and Hyperboloid have

Table 3. Evaluation of taxonomy link prediction in 32-d embedding spaces (16-d complex hyperbolic space for UnitBall). The best results are shown in boldface.

	ICD10				YAGO3-wikiObjects				WordNet-noun			
	MAP	MRR	Hits@1	Hits@3	MAP	MRR	Hits@1	Hits@3	MAP	MRR	Hits@1	Hits@3
Euclidean	3.75	3.72	0.26	2.39	4.85	4.45	0.62	2.78	5.59	5.36	0.31	3.16
Poincaré	35.24	34.45	6.68	52.71	30.06	28.47	10.84	41.61	25.46	23.99	7.56	27.80
Hyperboloid	34.80	34.01	6.01	52.88	30.80	29.21	11.81	43.17	25.65	24.15	7.52	27.50
UnitBall	47.88	46.96	24.24	70.28	33.33	31.85	15.62	47.41	27.29	25.93	10.42	32.95

Table 4. Evaluation of taxonomy link prediction in different embedding dimensions (the embedding dimension for UnitBall is half of other models). The best results are shown in boldface.

	ICD10						YAGO3-wikiObjects					
	8-dimensional			128-dimensional			8-dimensional			128-dimensional		
	MAP	MRR	Hits@3	MAP	MRR	Hits@3	MAP	MRR	Hits@3	MAP	MRR	Hits@3
Euclidean	2.57	2.57	1.32	10.83	10.48	4.66	1.02	0.92	0.57	16.67	15.76	15.97
Poincaré	35.73	34.94	53.10	34.47	33.70	52.19	29.70	28.13	41.64	29.93	28.35	41.53
Hyperboloid	35.56	34.77	51.90	34.93	34.15	52.98	30.87	29.28	43.50	30.68	29.07	42.86
UnitBall	44.05	43.26	61.54	46.54	45.59	70.03	31.40	29.98	44.25	32.76	31.28	46.25

very close performances, since they are both optimization-based learning algorithms in the hyperbolic space. TreeRep has comparable results with other methods when $(m, k) = (500, 1)$ since the graph is just a tree when $k = 1$, which is also revealed by the 0 δ -hyperbolicity in Figure 2. However, when $k > 1$ and $\delta > 0$, the graph becomes less tree-like, and TreeRep cannot achieve promising results, because when the data metrics deviate from tree metrics, it is not helpful to learn a tree from the data first.

5.3. Link Prediction

In this section, we evaluate the performances of UnitBall on the link prediction task for the real-world datasets. As our analysis in Section 5.2, TreeRep is not suitable for graphs that are not trees. Additionally, the large memory cost makes it unscalable to practical datasets. Therefore, we do not include TreeRep in the following experiments.

5.3.1. OVERALL RESULTS

Table 3 presents the results in 32-d embedding spaces for baselines and 16-d complex hyperbolic space for UnitBall. Predicting missing links is a much more difficult task than reconstructing graphs, but UnitBall still has the best performances on all three datasets. Besides, we see that Euclidean has unpromising results in the taxonomy datasets. Similar findings are shared in previous works on hyperbolic embeddings (Nickel & Kiela, 2017; Ganea et al., 2018), where the Euclidean space is demonstrated to be too flat and narrow for hierarchies. The hyperbolic embeddings (Poincaré and Hyperboloid) have significant improvements over the Euclidean embeddings, but they still fall behind UnitBall, which is consistent with our hypothesis that the non-constant negative curvature of complex hyperbolic space addresses

the varying hierarchical structures on real-world datasets.

5.3.2. EXPLORING THE EMBEDDING DIMENSIONS

We explore the performances in different embedding dimensions. The results on 8-d and 128-d embedding spaces (4-d and 64-d complex hyperbolic spaces for UnitBall) are presented in Table 4. We find that with the increase of the embedding dimension, Euclidean can have big improvements, but its performances in 128-d still cannot surpass the hyperbolic models in 8-d. By comparison, Poincaré, Hyperboloid, and UnitBall achieve great results steadily. 8-d is already enough for Poincaré and Hyperboloid to handle the link prediction task. In combination with the results in Table 3, we notice that UnitBall has small improvements from 4-d to 16-d, then converges to the stable performance. The results demonstrate that Euclidean models need to increase the dimension to better model the increasing complex hierarchies, while complex hyperbolic space and hyperbolic space have strong generalization competence for taxonomies.

6. Conclusion

In this paper, we present a novel approach for learning the embeddings of hierarchies in the unit ball model of complex hyperbolic space. We characterize the geometrical properties of complex hyperbolic space, including the variable negative curvature and the exponential growth of volume of geodesic balls, which are beneficial for data with various hierarchical structures. We exemplify the superiority of our approach over the graph reconstruction task and the link prediction task on both synthetic and real-world data. The empirical results show that our approach outperforms previous works on hyperbolic embeddings.

References

- Balazevic, I., Allen, C., and Hospedales, T. M. Multi-relational poincaré graph embeddings. In *NeurIPS*, pp. 4465–4475, 2019.
- Bécigneul, G. and Ganea, O. Riemannian adaptive optimization methods. In *ICLR (Poster)*. OpenReview.net, 2019.
- Bonnabel, S. Stochastic gradient descent on riemannian manifolds. *IEEE Trans. Autom. Control.*, 58(9):2217–2229, 2013.
- Bordes, A., Usunier, N., García-Durán, A., Weston, J., and Yakhnenko, O. Translating embeddings for modeling multi-relational data. In *NIPS*, pp. 2787–2795, 2013.
- Cannon, J. W., Floyd, W. J., Kenyon, R., Parry, W. R., et al. Hyperbolic geometry. *Flavors of geometry*, 31:59–115, 1997.
- Chami, I., Ying, Z., Ré, C., and Leskovec, J. Hyperbolic graph convolutional neural networks. In *NeurIPS*, pp. 4869–4880, 2019.
- Chami, I., Wolf, A., Juan, D., Sala, F., Ravi, S., and Ré, C. Low-dimensional hyperbolic knowledge graph embeddings. In *ACL*, pp. 6901–6914. Association for Computational Linguistics, 2020.
- Fu, R., Guo, J., Qin, B., Che, W., Wang, H., and Liu, T. Learning semantic hierarchies via word embeddings. In *ACL (1)*, pp. 1199–1209. The Association for Computer Linguistics, 2014.
- Ganea, O., Bécigneul, G., and Hofmann, T. Hyperbolic entailment cones for learning hierarchical embeddings. In *ICML*, volume 80 of *Proceedings of Machine Learning Research*, pp. 1632–1641. PMLR, 2018.
- Goldman, W. M. *Complex hyperbolic geometry*. Oxford University Press, 1999.
- Gromov, M. Hyperbolic groups. In *Essays in group theory*, pp. 75–263. Springer, 1987.
- Gu, A., Sala, F., Gunel, B., and Ré, C. Learning mixed-curvature representations in product spaces. In *ICLR (Poster)*. OpenReview.net, 2019.
- Krioukov, D., Papadopoulos, F., Kitsak, M., Vahdat, A., and Boguñá, M. Hyperbolic geometry of complex networks. *Phys. Rev. E*, 82:036106, Sep 2010. doi: 10.1103/PhysRevE.82.036106. URL <https://link.aps.org/doi/10.1103/PhysRevE.82.036106>.
- Linial, N., London, E., and Rabinovich, Y. The geometry of graphs and some of its algorithmic applications. *Combinatorica*, 15(2):215–245, 1995.
- Mahdisoltani, F., Biega, J., and Suchanek, F. M. YAGO3: A knowledge base from multilingual wikipeas. In *CIDR*. www.cidrdb.org, 2015.
- Miller, G. A. Wordnet: A lexical database for english. *Commun. ACM*, 38(11):39–41, 1995.
- Nickel, M. and Kiela, D. Poincaré embeddings for learning hierarchical representations. In *NIPS*, pp. 6338–6347, 2017.
- Nickel, M. and Kiela, D. Learning continuous hierarchies in the lorentz model of hyperbolic geometry. In *ICML*, volume 80 of *Proceedings of Machine Learning Research*, pp. 3776–3785. PMLR, 2018.
- Nickel, M., Tresp, V., and Kriegel, H. A three-way model for collective learning on multi-relational data. In *ICML*, pp. 809–816. Omnipress, 2011.
- Sala, F., Sa, C. D., Gu, A., and Ré, C. Representation tradeoffs for hyperbolic embeddings. In *ICML*, volume 80 of *Proceedings of Machine Learning Research*, pp. 4457–4466. PMLR, 2018.
- Sarkar, R. Low distortion delaunay embedding of trees in hyperbolic plane. In *Graph Drawing*, volume 7034 of *Lecture Notes in Computer Science*, pp. 355–366. Springer, 2011.
- Shwartz, V., Goldberg, Y., and Dagan, I. Improving hypernymy detection with an integrated path-based and distributional method. In *ACL (1)*. The Association for Computer Linguistics, 2016.
- Sonthalia, R. and Gilbert, A. C. Tree! I am no tree! I am a low dimensional hyperbolic embedding. In *NeurIPS*, 2020.
- Sun, Z., Deng, Z., Nie, J., and Tang, J. Rotate: Knowledge graph embedding by relational rotation in complex space. In *ICLR (Poster)*. OpenReview.net, 2019.
- Sun, Z., Chen, M., Hu, W., Wang, C., Dai, J., and Zhang, W. Knowledge association with hyperbolic knowledge graph embeddings. In *EMNLP (1)*, pp. 5704–5716. Association for Computational Linguistics, 2020.
- Trouillon, T., Welbl, J., Riedel, S., Gaussier, É., and Bouchard, G. Complex embeddings for simple link prediction. In *ICML*, volume 48 of *JMLR Workshop and Conference Proceedings*, pp. 2071–2080. JMLR.org, 2016.
- Yang, B., Yih, W., He, X., Gao, J., and Deng, L. Embedding entities and relations for learning and inference in knowledge bases. In *ICLR (Poster)*, 2015.
- Yu, T. and Sa, C. D. Numerically accurate hyperbolic embeddings using tiling-based models. In *NeurIPS*, pp. 2021–2031, 2019.